Published in final edited form as:
Circ Res. 2009 October 9; 105(8): 793–802. doi:10.1161/CIRCRESAHA.109.200568.

ALDOSE REDUCTASE PROTECTS AGAINST EARLY ATHEROSCLEROTIC LESION FORMATION IN APO E - NULL MICE

Sanjay Srivastava[a,*], **Elena Vladykovskaya**[a], **Oleg A. Barski**[a], **Matthew Spite**[a], **Karin Kaiserova**[a], **J. Mark Petrash**[b], **Stephen S Chung**[c], **Greg Hunt**[a], **Buddhadeb Dawn**[a], and **Aruni Bhatnagar**[a]

[a]Diabetes and Obesity Center, Institute of Molecular Cardiology, University of Louisville, Louisville, KY 40202

[b]Department of Ophalmology, Washington University, St. Louis, MO

[c]Department of Anatomy, University of Hong Kong, Hong Kong

Abstract

Rationale—Atherosclerotic lesion formation is associated with the accumulation of oxidized lipids. Products of lipid oxidation, particularly aldehydes, stimulate cytokine production and enhance monocyte adhesion, however their contribution to atherosclerotic lesion formation remains unclear.

Objective—To test the hypothesis that inhibition of aldehyde removal by aldose reductase (AR), which metabolizes both free and phospholipid aldehydes, would exacerbate atherosclerotic lesion formation.

Methods and Results—In atherosclerotic lesions of apoE-null mice, AR protein was localized with macrophage-rich regions and its abundance increased with lesion progression. Treatment of apoE-null mice with AR inhibitors sorbinil or tolrestat increased early lesion formation, but did not affect the formation of advanced lesions. Early lesions of $AR^{-/-}$/$apoE^{-/-}$ mice maintained on high fat diet were significantly larger when compared with age-matched $AR^{+/+}$/$apoE^{-/-}$ mice. The increase in lesion area due to deletion of the AR gene was seen in both male and female mice. Pharmacological inhibition or genetic ablation of AR also increased the lesion formation in male mice made diabetic by streptozotocin treatment. Lesions in $AR^{-/-}$/$apoE^{-/-}$ mice exhibited increased collagen and macrophage content and a decrease in smooth muscle cells. $AR^{-/-}$/$apoE^{-/-}$ mice displayed a greater accumulation of the AR substrate 4-hydroxy *trans*-2-nonenal (HNE) in the plasma and protein-HNE adducts in arterial lesions than $AR^{+/+}$/$apoE^{-/-}$ mice.

Conclusions—These observations indicate that AR is upregulated in atherosclerotic lesions and it protects against early stages of atherogenesis by removing toxic aldehydes generated in oxidized lipids.

Keywords

Lipid peroxidation; aldehydes; atherosclerosis; oxidative stress; macrophage

[*]Address correspondence to: Sanjay Srivastava, Ph.D., Division of Cardiovascular Medicine, Department of Medicine, Delia Baxter Building, 580 S. Preston St., Room 421B, University of Louisville, Louisville, KY 40202. Tel: (502) 852-5834; Fax: (502) 852-3663; sanjay@louisville.edu.

Disclosures: None

Introduction

Extensive evidence suggests that oxidation of lipoproteins that accumulate within the vessel wall is a significant feature of atherogenesis. In humans, the presence of oxidized lipids in the plasma and atherosclerotic lesions is strongly associated with coronary artery disease, acute coronary syndromes, and vulnerable plaques[1, 2]. In animal models, oxidized lipids have been detected in all stages of atherogenesis, and interventions that diminish lipid oxidation have been shown to decrease atherosclerotic lesion formation. Oxidizing lipids generate several bioactive molecules (e.g., alkoxyl and peroxyl radicals, peroxides, and isoprostanes), of which aldehydes are the major end products[3]. These aldehydes are generated from free radical-mediated scission of bis-allylic double bonds in unsaturated fatty acids, and they remain esterified to the phosphoglycerol backbone or to cholesterol or they appear as free carbonyls of varying chain lengths. Among the free and the esterified aldehydes generated during lipid oxidation, the C-9 unsaturated aldehyde, 4-hydroxy *trans*-2-nonenal (HNE) and the C-5 esterified aldehyde, 1-palmitoyl 2-oxovaleroyl phosphatidylcholine (POVPC) are the most abundant[2]. Protein adducts of HNE and POVPC have been detected in LDL oxidized *in vitro* [4] and in atherosclerotic lesions of animals[5] and humans[6], and positive reactivity of the plasma with anti-POVPC antibodies has been shown to correlate with lesion formation in apoE-null mice and with angiographically documented coronary artery disease in humans[7].

Aldehydes generated from oxidized lipids are highly reactive and they can increase monocyte adhesion, cytokine production[7] and trigger autophagy[8]. Multiple biochemical pathways have been identified that metabolize these aldehydes, and these pathways could potentially prevent aldehyde toxicity by converting them into less reactive products. Previous studies have led to the identification of the important role of paraoxonase[9] and platelet activating factor acyl hydrolase (PAF-AH)[2] in hydrolyzing oxidized *sn*-2 side chains of phospholipids and it has been shown that these enzymes protect against lesion development in atherosclerotic mice[9]. However, in addition to paraoxonase and PAF-AH, lipid-derived aldehydes are also reduced by aldose reductase (AR). AR is broad-specificity aldo-keto reductase and it is an efficient catalyst for the reduction of a range of free aldehydes generated from oxidized lipids. The enzyme also catalyzes the reduction of glutathione conjugates of unsaturated lipid-derived aldehydes[10] as well as POVPC and several related phospholipid aldehydes[11]. Nonetheless, the *in vivo* role of AR remains unclear. The current study was therefore designed to test the hypothesis that AR protects against atherosclerotic lesion formation by removing atherogenic lipid-derived aldehydes. Our results show that inhibition or genetic ablation of AR accelerates atherosclerotic lesion formation in apoE-null mice. These findings support the concept that aldehydes generated by oxidized lipids contribute to atherogenesis and that AR is a novel, and heretofore unrecognized, regulator of atherogenesis.

Methods

The $AR^{-/-}$/$apoE^{-/-}$ mice were generated by breeding $AR^{-/-}$ mice with $apoE^{-/-}$ mice. Mice underwent the treatment protocols described in Fig. 1. Plasma lipids were measured using commercial kits. Sorbitol concentration in the kidney was measured spectrofluorometrically. Expression of cytokines in the spleen was measured by quantitative PCR and plasma IL-6 levels were measured by ELISA.

Concentrations of aldehydes in the plasma were measured by gas chromatography-mass spectrometry (GC-MS). Atherosclerotic lesion area was calculated using Metamorph 4.5 software. Detailed Materials and Methods section is available as online supplement at http://circres.ahajournals.org.

Results

To understand the role of AR in atherogenesis, we first examined the association of this protein with atherosclerotic lesions. For this, apoE-null mice fed standard chow were euthanized at 8 and 20 weeks of age. As shown in Fig. 2A, in the innominate artery of 8-week old mice, the expression of AR was mostly co-localized with that of CD31, suggesting that in non-diseased tissue the AR gene is expressed mostly in endothelial cells. In agreement with previous findings with rat [12, 13] and human [14] vessels, no immunoreactivity with anti-AR antibody was associated with the medial smooth muscle cells, suggesting that non-activated smooth muscle cells do not express AR to the level observed in the endothelium. Lesions in the innominate artery of 20- week old mice were intensely stained with anti-AR antibody (Fig. 2B) and the expression of AR was co-localized with $CD68^+$ macrophages. The anti-AR antibody heavily stained the luminal surface of the lesion in the aortic sinus of 20-week old apoE-null mice (Fig 2C). The expression of AR in the aortic sinus co-localized with that of MOMA-2, suggesting that the enzyme may be specifically associated with macrophages accumulating in the sub-intimal space. The abundance of AR increased with lesion progression (Supplemental Fig. 1). Intense staining with the anti-AR antibody was observed in the aortic sinus of 52-week old mice and this staining co-localized with anti-MOMA-2 staining. These data demonstrate that although in non-diseased tissue the expression of AR is confined to the endothelium, the protein is abundant in the macrophage-rich regions of atherosclerotic lesions and its abundance increases with lesion progression.

To examine the contribution of AR to atherogenesis, we studied how treatment with AR inhibitors would affect different stages of atherogenesis in apoE-null mice. To assess the contribution of AR to early lesion formation, 8-week old mice were maintained on a high-fat diet and fed two structurally different AR inhibitors - tolrestat or sorbinil for 4 weeks in drinking water (*Protocol I*). At the end the study, the mice were euthanized and their plasma, kidney, heart and aorta were harvested. Sorbitol content of the kidney was measured to ensure the dose-efficacy of the AR inhibitors. In kidney, sorbitol is derived from AR-catalyzed reduction of glucose and tissue levels of sorbitol faithfully reflect cumulative AR activity. Our previous studies show that the changes in the levels of sorbitol in the aorta reflect those in the kidney[15]. Four-weeks of treatment with either tolrestat or sorbinil decreased sorbitol content in the kidney by 70–85 % (Supplemental Fig. 2). The extent of inhibition by the two drugs was similar, indicating that they were both equally effective in inhibiting AR *in situ* in apoE-null mice. Treatment with sorbinil or tolrestat, however, did not affect the plasma cholesterol and triglyceride concentrations (Supplemental Table 1) or distribution of cholesterol in the lipoproteins (data not shown). Treatment with sorbinil or tolrestat did not affect the body weight of the animals or their general health (data not shown). Based on these observations, we conclude that treatment with either tolrestat or sorbinil inhibits tissue AR activity but does not significantly affect plasma lipoprotein levels.

Morphometric analysis of the aortic roots showed that treatment with tolrestat led to a 1.9-fold increase in lesion formation when compared with vehicle-fed controls (Fig. 3A). Staining of the aortic sinus with oil red O showed small lipid-laden foam cells in the cusps of the aortic valves of vehicle-fed controls. Accumulation of cholesterol-rich foam cells was significantly increased in aortic roots of tolrestat-fed mice. Analysis of the aortic arch stained with Sudan IV showed a 2-fold increase in lesion area in tolrestat-fed mice versus vehicle-fed controls (Fig. 3B). Similar results were obtained with sorbinil. Morphometric analysis of the aortic root lesions of sorbinil-fed mice showed that the lesion size was 2.2-fold higher in sorbinil-treated mice when compared with vehicle-fed controls (Fig. 3 A). An increase of similar magnitude was observed in lesions in the aortic arch (Fig. 3 B). No

lesions were observed in the distal aorta of treated or untreated mice. Taken together, these data suggest that inhibition of AR accelerates early lesion formation in apoE-null mice.

We next examined whether inhibition of AR would affect lesion progression in the mice with pre-existing lesions. For these experiments, mice were maintained on the standard chow diet till they were 24 weeks of age. At this age, these mice show intermediate lesions throughout the vasculature. The mice were then fed either sorbinil (Protocol *IIB*) or vehicle II (*Protocol IIA*) for 12 weeks and euthanized when they were 36 weeks of age. Sorbinil feeding did not affect plasma cholesterol and triglycerides (Supplemental Table 1) in these mice. These mice developed advanced and complicated lesions; however, sorbinil treatment did not affect the extent of lesion formation either in the aortic root or in the abdominal aorta (Supplemental Fig. 3). These data suggest that inhibition of AR has no effect on the development of advanced lesions.

To further interrogate the role of AR in atherosclerotic lesion formation, we generated $AR^{-/-}/apoE^{-/-}$ mice. These mice were generated by breeding $AR^{-/-}$ mice (generated on C57 BL/6 background) with $apoE^{-/-}$ mice. The resulting $AR^{+/-}/apoE^{+/-}$ mice were inter-bred to generate $AR^{-/-}/apoE^{-/-}$ mice. The $AR^{-/-}/apoE^{-/-}$ mice maintained good general health and they bred normally. No change in the weight of their major organs was observed (data not shown). When 8-weeks of age, the $AR^{-/-}/apoE^{-/-}$ and their $AR^{+/+}/apoE^{-/-}$ littermates were maintained on high-fat diet for 4 (*Protocol III*) or 12 weeks (*Protocol IV*). No significant difference in the plasma cholesterol or triglyceride levels was observed between $AR^{-/-}/apoE^{-/-}$ and $AR^{+/+}/apoE^{-/-}$ mice (Supplemental Table 1). Western blot analysis of the heart homogenates confirmed the absence of AR protein in $AR^{-/-}/apoE^{-/-}$ (Fig. 4A). Morphometric analysis of the lesion area in the aortic sinus of the mice maintained on high-fat diet for 4 weeks showed that the mean lesion area of $AR^{-/-}/apoE^{-/-}$ was 2.2-fold higher than that of the $AR^{+/+}/apoE^{-/-}$ mice (Fig. 4B; $P<0.01$). A similar increase in lesion area was observed in the aortic arch of $AR^{-/-}/apoE^{-/-}$ when compared with $AR^{+/+}/apoE^{-/-}$ mice (Fig. 4C; $P<0.01$). At this age, no lesions were observed in the distal aorta of $AR^{-/-}/apoE^{-/-}$ or $AR^{+/+}/apoE^{-/-}$ mice (data not shown). These results, taken together with data obtained with AR inhibitors (Fig. 3), suggest that AR protects against early lesion formation in $apoE^{-/-}$ mice.

To examine the role of AR in intermediate lesion formation, $AR^{-/-}/apoE^{-/-}$ and $AR^{+/+}/apoE^{-/-}$ mice, maintained on high-fat diet for 12 weeks (*Protocol IV*), were used. Both male and female mice were used to elucidate gender-specific effects. Plasma cholesterol and triglyceride levels of $AR^{-/-}/apoE^{-/-}$ mice were comparable with $AR^{+/+}/apoE^{-/-}$ mice (Supplemental Table 1). The lesion area in the aortic sinus, aortic arch and abdominal aorta was 1.4 – 1.6-fold higher in the male $AR^{-/-}/apoE^{-/-}$ than in male $AR^{+/+}/apoE^{-/-}$ mice (Fig. 5A–C). When compared with male $AR^{+/+}/apoE^{-/-}$ mice, mean lesion area in female $AR^{+/+}/apoE^{-/-}$ mice was higher throughout the aortic tree. Lesion quantification in female $AR^{-/-}/apoE^{-/-}$ mice showed 1.6–1.9-fold increase (Fig. 5D–F) higher lesion area in aortic valves, aortic arch and the abdominal aorta, indicating that genetic ablation of AR enhances intermediate lesion formation and female $AR^{-/-}/apoE^{-/-}$ mice develop larger lesions than their male counterparts.

To examine lesion composition, sections of the aortic sinus of female $AR^{-/-}/apoE^{-/-}$ and $AR^{+/+}/apoE^{-/-}$ mice were stained with Sirius Red for collagen, α-smooth muscle cell actin for smooth muscle cells, CD-3 for T-lymphocytes and MOMA-2 for macrophages. As shown in Fig. 6A, the staining with Sirius Red showed that the interstitial collagen content of the lesions of $AR^{-/-}/apoE^{-/-}$ mice was 1.3-fold higher than $AR^{+/+}/apoE^{-/-}$mice ($P<0.05$). Staining for the smooth muscle cells showed that most of the smooth muscle cells were in the intimal area close to the lumen. The staining showed a 36% decrease in $AR^{-/-}/apoE^{-/-}$

when compared with $AR^{+/+}/apoE^{-/-}$mice (Fig. 6B; P<0.02). Only few cells (<2%) showed positive staining for T-lymphocytes. The extent of staining was similar in $AR^{-/-}/apoE^{-/-}$ and $AR^{+/+}/apoE^{-/-}$mice (data not shown). The macrophage content (probed with anti MOMA-2 antibody), in $AR^{-/-}/apoE^{-/-}$ mice was 1.7-fold greater than the lesions of $AR^{+/+}/apoE^{-/-}$ mice (Fig. 6C; P<0.01). Similarly a 1.4-fold increase in the number of $CD68^{+}$ macrophages in the aortic valves of $AR^{-/-}/apoE^{-/-}$ mice was observed (Fig. 6Di; P<0.02), however, there was no significant difference in the size of $CD68^{+}$ macrophages between the two groups (Fig. 6Dii). The expression of cytokines in the spleens of $AR^{-/-}/apoE^{-/-}$ mice was similar to $AR^{+/+}/apoE^{-/-}$mice (Supplemental Fig. 4A). Plasma concentration of IL-6 of $AR^{-/-}/apoE^{-/-}$ mice was also comparable to $AR^{+/+}/apoE^{-/-}$mice (Supplemental Fig. 4B). These observations suggest that genetic ablation of AR increases macrophage accumulation and interstitial fibrosis and decreases smooth muscle cell content of arterial lesions, without affecting systemic inflammation.

To examine whether the lack of AR prevents aldehyde removal, levels of the AR substrate HNE were measured in the plasma and protein-HNE adducts were quantified in arterial lesions. As shown in Fig. 7A, anti-protein-HNE antibody showed sparse immunopositive reactivity within the aortic root lesions of $AR^{+/+}/apoE^{-/-}$ mice. Confocal imaging showed weak staining with anti-protein-HNE antibody that was co-localized with the $CD68^{+}$ macrophages. The accumulation of protein-HNE adducts was markedly greater in the aortic roots of $AR^{-/-}/apoE^{-/-}$ mice versus $AR^{+/+}/apoE^{-/-}$. A distinct increase in the protein-HNE staining was also observed in the innominate arteries of $AR^{-/-}/apoE^{-/-}$ mice versus $AR^{+/+}/apoE^{-/-}$ (Supplemental Fig. 5A). Atherosclerotic lesions in innominate arteries also displayed marked immunoreactivity with another lipid peroxidation-derived aldehyde, malonaldialdehyde (MDA), which is not an AR substrate. No significant difference was observed in the protein-MDA staining in sections obtained from $AR^{-/-}/apoE^{-/-}$ and $AR^{+/+}/apoE^{-/-}$ lesions (Supplemental Fig. 5A). Similar results were obtained with plasma. Fig. 7B shows the chromatogram of the spectrum of PFB-oxime-TMS derivatives of HNE measured by gas chromatography-negative ionization chemical ionization mass spectrometry (GC-NICI-MS) by select ion monitoring mode, in the plasma of $AR^{+/+}/apoE^{-/-}$ and $AR^{-/-}/apoE^{-/-}$ mice (Fig. 7C). D_{11}-HNE was used as the internal standard. Following ions were monitored (Fig. 7C): D_{11}-HNE - m/z 294, 314 and 414 [M^{+}-$(CH_3)_3SiOH$-HFNO, M^{+}-$(CH_3)_3SiOH$-NO and M^{+}-HF] and HNE - m/z 283, 303 and 403 [M^{+}-$(CH_3)_3SiOH$-HFNO, M^{+}-$(CH_3)_3SiOH$-NO and M^{+}-HF]. The group data for the quantification of HNE is shown in Fig. 7D.

The plasma of $AR^{-/-}/apoE^{-/-}$ mice showed 2.5 -fold higher concentration of the AR substrate HNE than that of $AR^{+/+}/apoE^{-/-}$ mice (Fig. 7B–D). We also observed a significant increase in the plasma concentration of another AR substrate hexanal in $AR^{-/-}/apoE^{-/-}$ mice (data not shown). No difference in MDA levels was observed in the plasma of $AR^{-/-}/apoE^{-/-}$ versus $AR^{+/+}/apoE^{-/-}$ mice (Supplemental Fig. 5). These data suggest that in apoE-null mice deletion of the AR gene increases the accumulation of those aldehydes that are substrates of AR, without affecting the overall rate or extent of lipid peroxidation.

In addition to oxidized lipid-derived aldehydes, AR also catalyzes the metabolism of glucose. Therefore we also examined the role of AR during atherogenesis in diabetic apoE-null mice. Diabetes was induced by streptozotocin and lesion formation was examined after 6 or 12 weeks of diabetes (Protocol V). As shown in Fig. 8, in the diabetic mice, inhibition of AR by sorbinil increased the lesion formation by 1.6-fold (Fig. 8A; P<0.02) in the aortic valve and 1.8 fold in the aortic arch (Supplemental Fig. 6). Sorbinil feeding had no effect on plasma cholesterol and triglyceride concentrations (Supplemental Table 1). Similar to pharmacological inhibition, genetic ablation of AR also increased lesion formation in diabetic mice. After 6 weeks of diabetes, the surface lesion area of $AR^{-/-}/apoE^{-/-}$ mice was

1.6-fold larger in the aortic valve (P<0.02; Fig. 8B) and 1.7-fold larger in the aortic arch (P<0.02; Supplemental Fig. 6B) as compared with $AR^{+/+}/apoE^{-/-}$ mice. No significant difference was observed in the plasma cholesterol and triglyceride concentrations between $AR^{-/-}/apoE^{-/-}$ and $AR^{+/+}/apoE^{-/-}$ mice. After 12 weeks of diabetes the lesion area in the aortic valve of $AR^{-/-}/apoE^{-/-}$ mice was 1.4-fold higher than $AR^{+/+}/apoE^{-/-}$ mice (Fig. 8C; P<0.05) whereas plasma cholesterol and triglyceride concentrations between the two strains of mice were comparable. A more pronounced increase in the lesion area of the aortic arch (1.7- fold) and the abdominal aorta (2-fold) was observed in the $AR^{-/-}/apoE^{-/-}$ mice as compared with $AR^{+/+}/apoE^{-/-}$ mice (Supplemental Fig. 6B). These data suggest that as in non-diabetic mice, inhibition of AR increases atherogenesis in diabetic apoE-null mice.

Discussion

The major finding of this study is that inhibition of AR exacerbates atherosclerotic lesion formation in non-diabetic and diabetic apoE null mice. This finding support the concept that aldehydes generated by lipid peroxidation promote atherogenesis and that the processes involved in detoxifying these aldehydes may be significant modulators of atherogenesis. The observation that inhibition of AR increases and accelerates the formation of early and intermediate lesions, but does not affect the progression of pre-formed plaques indicates that aldehyde metabolism by AR may be particularly significant during the early stages of lesion formation. Acceleration of atherogenesis in mice treated with AR inhibitors was not associated with significant changes in plasma lipoprotein levels but with an increase in the accumulation of protein-HNE adducts within the aortic lesions, suggesting that inhibition by AR does not ameliorate systemic dyslipidemia but rather it promotes the accumulation of lipid peroxidation-derived aldehydes within the vessel wall.

Extensive evidence supports the concept that AR is a critical participant in the metabolism and detoxification of aldehydes derived from lipid peroxidation. The catalytic cycle, the active site, and the energetics of the enzyme are optimized for the removal of variety of endogenous aldehydes ranging from saturated and unsaturated aldehydes, phospholipid aldehydes, steroid aldehydes, 2-oxo-aldehydes and base propenals [16]. Because most of these aldehydes are highly reactive and are generated endogenously during oxidative stress, their reduction by AR could be considered to be an antioxidant defense mechanism. Consistent with this role, AR has been found to be increased by oxidative stress induced by hydrogen peroxide, HNE, NO, methylglyoxal, or iron overload [16]. The levels of AR are also elevated during oxidative stress *in vivo* in myocardial ischemia-reperfusion[17], restenosis[12], vasculitis[14], and atherogenesis (this study; Fig. 2). Moreover, it has been recently shown that the *ar* gene is transcriptionally upregulated by the binding of Nrf2 to the antioxidant response element at the 5'-flanking region of the AR gene[18], and that during myocardial ischemia AR is activated by post-translational modification of its cysteine residues to sulfenic acid[19]. Transcriptional and post-translational increases during oxidative stress indicate that AR may be an important component of the antioxidant response specifically upregulated to prevent aldehyde toxicity. This role of AR is in agreement with previous reports showing that inhibition of AR increases the toxicity of aldehydes such as HNE[20], acrolein, and glycoaldehyde[21] and promotes aldehyde accumulation in inflamed arteries[14] or the ischemic heart[17]. Thus, elevated levels of AR seen in atherosclerotic lesions in the current study support the idea that the accumulation of lipid peroxidation products is a significant cause of oxidative stress in atherosclerotic lesions and that AR prevents lesion formation by mitigating their toxicity. Significantly, we found that deletion of AR increased the levels of HNE and hexanal in the plasma and the protein-HNE in the lesions, without affecting plasma MDA levels or the abundance of protein-MDA adducts in the lesions. These observations suggest that loss of AR does not lead to a systemic increase in lipid

peroxidation or oxidative stress (because levels of MDA were not affected), but that it prevents the removal of only those aldehydes that are AR substrates (i.e., HNE and hexenal).

Accumulation of oxidized lipids in the sub-intimal space is believed to be an initiating event in atherogenesis[2]. Although LDL in its native form is not atherogenic, oxidation in the acellular regions of the vessel wall transforms the particle into an inflammatory trigger and a high affinity ligand of the scavenger receptor. In support of this view it has been shown that oxidized LDL induces the synthesis of cytokines and chemokines such as MCP-1 and IL-8 and that it could recruit inflammatory cells to the lesion by promoting endothelial-monocyte adhesion[1, 2]. Several of the atherogenic properties of oxidized LDL have been linked to the generation of lipid peroxidation-derived aldehydes such as HNE and POVPC[1, 2], which are substrates of AR. Hence reduction by AR, which coverts the reactive aldehyde function to an alcohol could reduce toxicity and thereby prevent the activation of the processes by which aldehydes generated in oxidized LDL contribute to lesion progression. In agreement with the view that reduction decreases the bioactivity of lipid-derived aldehydes it has been shown that chemical reduction of POVPC abolishes its ability to promote the binding of monocytes to the endothelium[22], suggesting that the metabolic transformation by AR could decrease the bioactivity as well as the atherogenic effects of lipid-derived aldehydes.

The notion that AR is a major determinant of aldehyde metabolism in vascular lesions is consistent with our observation that inhibition of AR increases the accumulation of protein-aldehyde adducts in the lesion and accelerates the formation of early and intermediate lesions. Nevertheless, the possibility that alcohol products of lipid peroxidation could retain or enhance the biological activity of the aldehydes could not be ruled out. Indeed, our studies show that in smooth muscle cells, AR is essential for the activation of NF-κB by growth factors and cytokines[16, 23] and that reduction of glutathionyl-HNE by AR is an activating step in HNE metabolism which is required for NF-κB activation and for stimulation of smooth muscle cell growth[24]. The mechanisms which impart a dual role to AR are unclear, but it appears likely that the pro- and anti-inflammatory roles of AR depend upon the metabolic context. A similar duality of function is associated with NF-κB, which is regulated by AR[23]. Activated NF-κB has been detected in macrophages, smooth muscle cells and endothelial cells of atherosclerotic lesions and lesion prone sites[25], however, inhibition of NF-κB in macrophage increases atherosclerosis and lesion inflammation[26]. Thus, reduction of aldehydes and their glutathione conjugates by AR could be beneficial under some conditions but not others. Indeed, the complex role of AR is highlighted by the contrast between the findings of our current study and those of Vikramadithyan *et al.*, who reported that general transgenic overexpression of AR driven by a mouse histocompatability antigen class I promoter *increased* the formation of atherosclerotic lesions in streptozotocin-treated diabetic LDL-receptor null mice without affecting lesion formation in non-diabetic mice[27]. In contrast our results show that genetic ablation or pharmacological inhibition of AR increases lesion formation in both diabetic and non-diabetic mice. It is possible that the expression of the AR transgenic in tissues, where AR is not basally expressed (for example, vascular smooth muscle cells and liver) could artificially affect lesion formation by inducing non-specific changes in other genes due to constitutive overexpression of AR. Our results (Figure 2) show that AR is mostly associated with atherosclerotic lesions and thus a basal level of expression of AR in tissues where it is not expressed (e.g., smooth muscle cells) could artificially promote lesion formation (AR is a critical regulator of vascular smooth muscle cells and neointima formation)[12, 13]. In this regard, our data showing similar effects due to a loss of AR catalysis during lesion formation (by pharmacological inhibition) or constitutive deletion of the AR gene both in diabetic and non-diabetic mice provide consistent evidence that AR prevents the formation of early and intermediate lesions. This is important because AR inhibitors have been suggested to be potential therapeutic agents for the treatment of secondary diabetic complications[16].

Our finding that inhibition of aldehyde metabolism promotes atherosclerotic lesions formation provides further support to the concept that lipoprotein oxidation is a critical regulator of atherogenesis. Although, oxidized lipids and their electrophilic components have been shown to induce a variety of atherogenic effects in cell culture systems, direct *in vivo* evidence implicating their involvement in lesion formation is lacking. Hence, our studies showing that inhibition of metabolism and detoxification of at least one component of oxidized lipids aggravates lesion formation provides the first line of evidence that in addition to being foot prints of oxidative stress, aldehydes derived from lipid peroxidation play a direct role in atherosclerosis. Results of lesion analysis show loss of AR is associated with an increase in collagen deposition and a decrease in smooth muscle cell content. This is surprising because collagen deposition in plaques and the formation of a fibrous cap have been linked to smooth muscle cells in the lesoin. However, our previous work shows that AR is essential for smooth muscle cell growth in culture[12] and that inhibition of AR prevents neo-intima formation in injured arteries[13]. However, the loss of AR, which results in the accumulation of its substrate HNE in the lesion could increase profibrogenic activity[28]. It has been shown that HNE induces TGFβ1 and activtates AP-1 thereby increasing collagen synthesis[29].

The observation that inhibition of AR prevents the formation of early and intermediate, but not late lesions is consistent with the current view of the role of oxidative stress in atherosclerosis. Recruitment of monocytes and the formation of foam cells are early events that are most likely triggered by oxidized components of LDL, whereas during later stages of lesion formation, the production of cytokines and inflammatory circuits within the vessels may be self-sustaining. The insensitivity of late lesion to AR inhibition is consistent with this view and suggests that lipid peroxidation products differentially play a more important role during the early than during the advanced stages of plaque generation.

In summary, we have found that inhibition of AR exacerbates atherosclerotic lesion formation and promotes vascular accumulation of protein-aldehyde adducts in apoE-null mice without affecting plasma lipoproteins. These observations support the concept that aldehydes-derived from lipid peroxidation play a central causal role in the formation and the progression of aortic lesions and that processes that prevent the accumulation and the toxicity of lipid-derived aldehydes may be beneficial in preventing or diminishing plaque burden. The observations reported here highlight on one hand the need for additional mechanistic studies to delineate the role of aldehyde metabolism in regulating vascular inflammation, cholesterol uptake, and lesion formation, and on the other, the necessity of additional molecular epidemiological studies to assess whether inter-individual or polymorphic changes in the genes for AR (or other aldehyde-metabolizing enzymes) regulate the overall risk of cardiovascular disease in human populations.

Materials and Methods

Animal housing and treatment protocols

The mice were housed under pathogen-free conditions in the University of Louisville vivarium under controlled temperature and 12 h light/12 h dark cycle. Prior to the indicated protocols, all the mice were maintained on a standard chow diet (PicoLab Rodent Chow 20 containing 4.5 % fat by weight and 0.02 % cholesterol).

The $AR^{+/+}$/$apoE^{-/-}$ mice (B6.129P2-*Apoe*^{tm1Unc}/J) were obtained from Jax Labs, Bar Harbor, ME. The $AR^{-/-}$/$apoE^{-/-}$ mice were generated by breeding $AR^{-/-}$ mice (on C57 BL/6 background)[1] with $apoE^{-/-}$ mice. The resulting heterozygous progengy were interbred with each other to produce homozygote $AR^{-/-}$/$apoE^{-/-}$ mice. To identify the apoE genotype following set of primers were used: F: 5'-GCCTAGCCGAGGGAGAGCCG-3'; R(WT): 5'-

TGTGACTTGGGAGCTCTGCAGC-3' and R(knock out): 5'-GCCGCCCCGACTGCATCT-3'. For genotyping AR, following 3 primers were used[2]: F(WT): 5'-GGGCTATACGGAGAAACTGTGT-3'; F(knock out): 5'-ATCAGCAGCCTCTGTTCCAC-3' and R: 5'-TGACCTTCCTCTAGAGGCTCTT-3'. Expression of AR protein (in the heart) was examined by Western blotting, using anti-AR antibody (Fig. 4A).

Four groups of mice underwent the following treatment protocols (Scheme I). In *Protocol I*, 8 week old mice (n=40) were divided into 4 sub groups (*Protocol IA – D*). Mice in *Protocol I*, were fed AR inhibitors-tolrestat (0.2 g/L in 2.5 mM sodium bicarbonate in drinking water; *Protocol IB*; n=10) or sorbinil (0.2g/L in 0.5 % ethanol in drinking water; *Protocol ID*; n=10) for 4 weeks. Mice fed with the vehicle, 2.5 mM sodium bicarbonate in drinking water (*vehicle I; Protocol IA*; n=10) or 0.5 % ethanol in drinking water (*vehicle II; Protocol IC*; n=10), were used as controls for the tolrestat- and sorbinil-fed mice, respectively. Mice treated according to *Protocol IA – D* were fed a high-fat (HF) Western-style diet (Teklad TD 88137 containing 21.2% fat and 4.5% cholesterol). In *Protocol II*, 24-week old mice were fed sorbinil (*Protocol IIIB*; n=12) or *vehicle II* (*Protocol IIIA*; n=12) for 12 weeks and maintained on standard rodent chow diet. In *Protocol III*, 8 week old male, $AR^{+/+}/apoE^{-/-}$ (*Protocols IIIA*; n=10) and $AR^{-/-}/apoE^{-/-}$ (*Protocols IIIB*; n=10) mice were fed high fat/high cholesterol western style diet for 4 weeks. In *Protocol IV*, 8-week old, male $AR^{+/+}/apoE^{-/-}$ (*Protocols IVA*; n=10) and $AR^{-/-}/apoE^{-/-}$ (*Protocols IVB*; n=10) and female $AR^{+/+}/apoE^{-/-}$ (*Protocols IVC*; n=10) and $AR^{-/-}/apoE^{-/-}$ (*Protocols IVD*; n=10) mice were fed high-fat/high cholesterol western-style diet for 12 weeks.

To examine the effect of AR inhibitors on atherogenesis in diabetic mice, 6-week old apoE-null mice, maintained on normal chow, were administered 6 daily intraperitoneal injections of streptozotocin (65 mg/kg/day, *Protocol V*)[3]. After 2 weeks, mice with blood glucose level > 250 mg/dL were divided in two sub groups. Mice in group VB were fed sorbinil (0.2g/L; n=10) in drinking water and mice in group *VA* were fed with vehicle (0.1 % ethanol; n=10). Mice were maintained on normal chow for 6 weeks and then euthanized to quantify the lesion formation. To examine the effect of genetic ablation of AR on atherosclerotic lesion formation, diabetes was induced in $AR^{+/+}/apoE^{-/-}$ and $AR^{-/-}/apoE^{-/-}$ mice as described above. Mice were maintained on normal chow and euthanized after 6 (*Protocol VC* and *VD*; n=10/group) or12 (*Protocol VE* and *VF*; n=10/group) weeks of diabetes to quantify lesion formation.

One mouse in *Protocol IIB*, died prior to completion of the treatment regime and was excluded from the study. All the other mice completed the experimental protocol successfully. At the end of the treatment protocol, mice were anesthetized with pentobarbital (150 mg/Kg) and blood and tissues were removed and used as described below.

Plasma lipoprotein analyses

After anesthesia the mice were bled (using 3mM di-sodium EDTA as anti-coagulant) by cardiac puncture. Blood was centrifuged at 300×*g* for 10 min at room temperature. The supernatant was aspirated and centrifuged at 13000×*g* for 10 min at 4 ºC to obtain clear plasma. Plasma cholesterol and triglycerides levels were measured using commercial kits from Wako Chemicals Inc. (Ritchmond, VA) as per manufacturer's instructions. Cholesterol distribution in the lipoproteins was assessed by size-exclusion chromatography using a Superose 6B column (Pharmacia LKB Biotechnology Inc). The column was eluted with 10 mM potassium phosphate, pH 7.4 containing 150 mM sodium chloride and 0.05% sodium azide, at a flow rate of 0.5 ml/min and cholesterol in each fraction was measured using the Wako kit.

Measurement of sorbitol

To examine the efficacy of tolrestat and sorbinil in inhibiting AR *in vivo*, sorbitol concentration in the kidney was measured as described[4]. Briefly, frozen kidneys were pulverized in liquid nitrogen and homogenized in 4 volumes of 6% perchloric acid. Homogenates were centrifuged at 2,400×*g* for 10 min at 4 °C and the protein-free supernatant (1.0 ml) was mixed with 0.5 ml of glycine buffer (pH 9.4) containing 3.6 mM NAD^+ and 6 units of sorbitol dehydrogenase and sorbitol concentration was measured spectrofluorometrically[4].

Quantification of cytokines

Pro-inflammatory cytokines were measured in the spleen in *Protocol IV* animals. Spleens were snap-frozen immediately after harvesting. RNA was isolated using Trizol reagent and 2.0 μg RNA from each was reverse transcribed with AMV reverse transcriptase (Promega Corp., Madison, WI) at 42°C for 60 min, followed by PCR amplification. Quantitative RT-PCR was carried out in a BioRad Real Time PCR thermocycler using SYBR green/ Fluorescein PCR master mix (SuperArray Biosciences Corp., Frederick, MD). Following primers were used: TNF-α – F:GCATGATCCGCGACGTGGAA and R: AGATCCATGCCGTTGGCCAG; IL-1β - F:CTCCATGAGCTTTGTACAAGG and R: TGCTGATGTACCAGTTGGGG; GAPDH – F:AGGTCATCCCAGAGGTGAACG and R: GGAGTTGCTGTTGAAGTCGCA. For IL-6 measurement a commercial set of primers from SuperArray Biosciences was used. Concentration of IL-6 in the plasma was measured by ELISA.

Measurements of aldehydes by gas chromatography-mass spectrometry

Concentrations of HNE and MDA were measured as described before [5, 6]. D_{11}-HNE was used as internal standard to quantify HNE and benzaldehyde ring D_5 was used as internal standard for the quantification of MDA.

Atherosclerotic lesion analyses

For the morphometric analysis, entire aorta from the heart, extending to the iliac arteries and including the subclavian right and left common carotid arteries, was removed and rinsed with phosphate-buffer saline (PBS). Peri-adventetial tissue was removed under the dissecting microscope and wherever indicated, aortic arch and the distal aorta were cut longitudinally to expose the intimal surface. The tissue was pinned *en face* on wax and the lipids were stained with Sudan IV, wherever indicated. The aortic arch was defined as the region from ascending arch to 3 mm distal to subclavial artery[7]. Percent lesion area was calculated using Metamorph 4.5 software.

For the analysis of lesion formation in the aortic sinus, the tissue was frozen in OCT reagent and serial cryosections of 8 μm-thickness were taken from the origin of the aortic valve leaflets, throughout the aortic sinus as described by Paigen *et al.*[8]. Mean lesion area was calculated from the analysis of digital images obtained from 9–12 serial section from each mouse, using Metamorph 4.5 software. Oil red O staining was used to detect the lipid deposition in these sections. Sirius Red staining was used to visualize collagen.

Immunohistochemical analyses

Polyclonal anti-AR antibody was raised in rabbit as described before[9]. Macrophages were detected with a rat monoclonal antibody against mouse macrophages, clone MOMA-2 (Serotec, Raleigh, NC); smooth muscle cells were identified with a monoclonal anti-α-smooth muscle cell actin, clone A4 (Sigma Chemicals, St. Louis, MO) and T-lymphocytes were stained with a rabbit polyclonal anti-CD3 antibody (Santa Cruz Biotechnology, Santa

Cruz, CA). Air-dried cryostat sections were fixed in cold acetone for 2h and the endogenous peroxidase activity was quenched with 3% hydrogen peroxide. After incubation with appropriate primary and secondary antibodies, the immunostains were visualized with Nova Red (Vector Laboratories). The sections were then conterstained with Mayer's hematoxylin, wherever indicated. Protein-MDA staining in the sections of formalin fixed innominate arteries were done as descibed before [10]. At least three sections per animal were analyzed for each staining. For polyclonal antibodies, non-immune serum was used in place of the primary antibody as a negative control. For the monoclonal antibodies, sections untreated with primary antibody served as control. Digital images were acquired using Spot advanced camera and analyzed by Metamorph 4.5 software as described[9, 10]. For each stain, the threshold was predetermined, and held constant for all sections analyzed from each protocol. The samples were analyzed by one blinded observer.

Immunofluorescence Staining and Confocal Microscopy

Sections of the innominate artery and aortic sinus were stained with Alexa 647-conjugated rat anti-mouse CD68 (Serotec, Raleigh, NC; 1:150, overnight at 4° C). Nuclei were stained with DAPI. For staining CD31, MOMA-2, AR and protein-HNE, samples were incubated with the primary antibody as follows: CD31(Biocare Medical, Concord, CA; 1:150, 1h room temperature), MOMA-2 (Serotec, Raleigh, NC; 1:25, overnight), AR[9] (1:200; overnight) and protein (KLH)-HNE [9] (1:200; overnight). Sections stained with non-immune mouse or rabbit IgG were used as negative controls. Samples were then incubated with TRITC or Alexa-488 labeled appropriate secondary antibodies. Confocal images were acquired within 6h of staining on a Zeiss LSM 510 microscope (Zeiss, Oberkochen, Germany).

Statistical analyses

All results are presented as mean ± standard error of mean (SEM). Data were analyzed by Student's *t* test. A value of $P<0.05$ was considered significant.

Supplementary Material

Refer to Web version on PubMed Central for supplementary material.

Acknowledgments

The authors are thankful to Ms. Barbara Bishop, Mr. David Young and Ms. Erica Werkman for expert technical assistance.

Sources of Funding: This work was supported in part by NIH grants ES17260, ES11594, ES11860, HL55477, HL59378 EY5856 and RR 24489.

Non-standard Abbreviations and Non-Standard Acronyms

(HNE)	4-Hydroxy *trans*-2-nonenal
POVPC	1-palmitoyl 2-oxovaleroyl phosphatidylcholine
MDA	malonaldialdehyde
AR	aldose reductase

References

1. Berliner JA, Subbanagounder G, Leitinger N, Watson AD, Vora D. Evidence for a role of phospholipid oxidation products in atherogenesis. Trends Cardiovasc Med. 2001; 11:142–147. [PubMed: 11686004]

2. Stocker R, Keaney JF Jr. Role of oxidative modifications in atherosclerosis. Physiol Rev. 2004; 84:1381–1478. [PubMed: 15383655]
3. Esterbauer H, Schaur RJ, Zollner H. Chemistry and biochemistry of 4-hydroxynonenal, malonaldehyde and related aldehydes. Free Radic Biol Med. 1991; 11:81–128. [PubMed: 1937131]
4. Requena JR, Fu MX, Ahmed MU, et al. Quantification of malondialdehyde and 4-hydroxynonenal adducts to lysine residues in native and oxidized human low-density lipoprotein. Biochem J. 1997; 322:317–325. [PubMed: 9078279]
5. Rosenfeld ME, Palinski W, Yla-Herttuala S, Butler S, Witztum JL. Distribution of oxidation specific lipid-protein adducts and apolipoprotein B in atherosclerotic lesions of varying severity from WHHL rabbits. Arteriosclerosis. 1990; 10:336–349. [PubMed: 1693069]
6. Jurgens G, Chen Q, Esterbauer H, Mair S, Ledinski G, Dinges HP. Immunostaining of human autopsy aortas with antibodies to modified apolipoprotein B and apoprotein(a). Arterioscler Thromb. 1993; 13:1689–1699. [PubMed: 7692957]
7. Tsimikas S, Brilakis ES, Miller ER, et al. Oxidized phospholipids, Lp(a) lipoprotein, and coronary artery disease.[see comment]. New Engl J Med. 2005; 353:46–57. [PubMed: 16000355]
8. Hill BG, Haberzettl P, Ahmed Y, Srivastava S, Bhatnagar A. Unsaturated lipid peroxidation-derived aldehydes activate autophagy in vascular smooth-muscle cells. Biochem J. 2008; 410:525–534. [PubMed: 18052926]
9. Shih DM, Xia YR, Wang XP, Miller E, Castellani LW, Subbanagounder G, Cheroutre H, Faull KF, Berliner JA, Witztum JL, Luisis AJ. Combined serum paraoxonase knockout/apolipoprotein E knockout mice exhibit increased lipoprotein oxidation and atherosclerosis. J Biol Chem. 2000; 275:17527–17535. [PubMed: 10748217]
10. Srivastava S, Watowich SJ, Petrash JM, Srivastava SK, Bhatnagar A. Structural and kinetic determinants of aldehyde reduction by aldose reductase. Biochemistry. 1999; 38:42–54. [PubMed: 9890881]
11. Srivastava S, Spite M, Trent JO, West MB, Ahmed Y, Bhatnagar A. Aldose reductase-catalyzed reduction of aldehyde phospholipids. J Biol Chem. 2004; 279:53395–53406. [PubMed: 15465833]
12. Ruef J, Liu SQ, Bode C, et al. Involvement of aldose reductase in vascular smooth muscle cell growth and lesion formation after arterial injury. Arterioscler Thromb Vasc Biol. 2000; 20:1745–1752. [PubMed: 10894812]
13. Srivastava S, Ramana KV, Tammali R, Srivastava SK, Bhatnagar A. Contribution of aldose reductase to diabetic hyperproliferation of vascular smooth muscle cells. Diabetes. 2006; 55:901–910. [PubMed: 16567509]
14. Rittner HL, Hafner V, Klimiuk PA, Szweda LI, Goronzy JJ, Weyand CM. Aldose reductase functions as a detoxification system for lipid peroxidation products in vasculitis. J Clin Invest. 1999; 103:1007–1013. [PubMed: 10194473]
15. Chandra D, Jackson EB, Ramana KV, Kelley R, Srivastava SK, Bhatnagar A. Nitric oxide prevents aldose reductase activation and sorbitol accumulation during diabetes. Diabetes. 2002; 51:3095–3101. [PubMed: 12351453]
16. Srivastava SK, Ramana KV, Bhatnagar A. Role of aldose reductase and oxidative damage in diabetes and the consequent potential for therapeutic options. Endocr Rev. 2005; 26:380–392. [PubMed: 15814847]
17. Shinmura K, Bolli R, Liu SQ, et al. Aldose reductase is an obligatory mediator of the late phase of ischemic preconditioning. Circ Res. 2002; 91:240–246. [PubMed: 12169650]
18. Nishinaka T, Yabe-Nishimura C. Transcription factor Nrf2 regulates promoter activity of mouse aldose reductase (AKR1B3) gene. J Pharmacol Sci. 2005; 97:43–51. [PubMed: 15655294]
19. Kaiserova K, Srivastava S, Hoetker JD, et al. Redox activation of aldose reductase in the ischemic heart. J Biol Chem. 2006; 281:15110–15120. [PubMed: 16567803]
20. Yadav UC, Ramana KV, Awasthi YC, Srivastava SK. Glutathione level regulates HNE-induced genotoxicity in human erythroleukemia cells. Toxicol Appl Pharmacol. 2008; 227:257–264. [PubMed: 18096195]
21. Keightley JA, Shang L, Kinter M. Proteomic analysis of oxidative stress-resistant cells: a specific role for aldose reductase overexpression in cytoprotection. Mol Cell Proteomics. 2004; 3:167–175. [PubMed: 14676331]

22. Subbanagounder G, Leitinger N, Schwenke DC, et al. Determinants of bioactivity of oxidized phospholipids. Specific oxidized fatty acyl groups at the sn-2 position. Arterioscler Thromb Vasc Biol. 2000; 20:2248–2254. [PubMed: 11031211]

23. Ramana KV, Chandra D, Srivastava S, Bhatnagar A, Aggarwal BB, Srivastava SK. Aldose reductase mediates mitogenic signaling in vascular smooth muscle cells. J Biol Chem. 2002; 277:32063–32070. [PubMed: 12063254]

24. Ramana KV, Bhatnagar A, Srivastava S, Yadav UC, Awasthi S, Awasthi YC, Srivastava SK. Mitogenic responses of vascular smooth muscle cells to lipid peroxidation-derived aldehyde 4-hydroxy-trans-2-nonenal (HNE): role of aldose reductase-catalyzed reduction of the HNE-glutathione conjugates in regulating cell growth. J Biol Chem. 2006; 281:17652–17660. [PubMed: 16648138]

25. de Winther MP, Kanters E, Kraal G, Hofker MH. Nuclear factor kappaB signaling in atherogenesis. Arterioscler Thromb Vasc Biol. 2005; 25:904–914. [PubMed: 15731497]

26. Kanters E, Pasparakis M, Gijbels MJ, Vergouwe MN, Partouns-Hendriks I, Fijneman RJ, Clausen BE, Forster I, Kockx MM, Rajewsky K, Kraal G, Hofker MH, de Winther MP. Inhibition of NF-kappaB activation in macrophages increases atherosclerosis in LDL receptor-deficient mice. J Clin Invest. 2003; 112:1176–1185. [PubMed: 14561702]

27. Vikramadithyan RK, Hu Y, Noh HL, Liang CP, Hallam K, Tall AR, Ramasamy R, Goldberg IJ. Human aldose reductase expression accelerates diabetic atherosclerosis in transgenic mice. J Clin Invest. 2005; 115:2434–2443. [PubMed: 16127462]

28. Chiarpotto E, Catello L, Leonarduzzi G, Biasi AF, Poli G. Role of 4-hydroxy-2,3-nonenal in the pathogenesis of fibrosis. Biofactors. 2005; 24:229–236. [PubMed: 16403983]

29. Chiarpotto E, Bergamini E, Poli G. Molecular mechanisms of calorie restriction's protection against age-related sclerosis. IUBMB Life. 2006; 58:695–702. [PubMed: 17424908]

1. Ho HT, Chung SK, Law JW, Ko BC, Tam SC, Brooks HL, Knepper MA, Chung SS. Aldose reductase-deficient mice develop nephrogenic diabetes insipidus. Mol Cell Biol. 2000; 20:5840–5846. [PubMed: 10913167]

2. Yang JY, Tam WY, Tam S, Guo H, Wu X, Li G, Chau JF, Klein JD, Chung SK, Sands JM, Chung SS. Genetic restoration of aldose reductase to the collecting tubules restores maturation of the urine concentrating mechanism. Am J Physiol Renal Physiol. 2006; 291:F186–F195. [PubMed: 16449351]

3. Park L, Raman KG, Lee KJ, Lu Y, Ferran LJ Jr, Chow WS, Stern D, Schmidt AM. Suppression of accelerated diabetic atherosclerosis by the soluble receptor for advanced glycation endproducts. Nat Med. 1998; 4:1025–1031. [PubMed: 9734395]

4. Kaiserova K, Srivastava S, Hoetker JD, Awe SO, Tang XL, Cai J, Bhatnagar A. Redox activation of aldose reductase in the ischemic heart. J Biol Chem. 2006; 281:15110–15120. [PubMed: 16567803]

5. Shinmura K, Bolli R, Liu SQ, Tang XL, Kodani E, Xuan YT, Srivastava S, Bhatnagar A. Aldose reductase is an obligatory mediator of the late phase of ischemic preconditioning. Circ Res. 2002; 91:240–246. [PubMed: 12169650]

6. Srivastava S, Chandrasekar B, Bhatnagar A, Prabhu SD. Lipid peroxidation-derived aldehydes and oxidative stress in the failing heart: role of aldose reductase. Am J Physiol Heart Circ Physiol. 2002; 283:H2612–H2619. [PubMed: 12388223]

7. Webb NR, Bostrom MA, Szilvassy SJ, van der Westhuyzen DR, Daugherty A, de Beer FC. Macrophage-expressed group IIA secretory phospholipase A2 increases atherosclerotic lesion formation in LDL receptor-deficient mice. Arterioscler Thromb Vasc Biol. 2003; 23:263–268. [PubMed: 12588769]

8. Paigen B, Morrow A, Holmes PA, Mitchell D, Williams RA. Quantitative assessment of atherosclerotic lesions in mice. Atherosclerosis. 1987; 68:231–240. [PubMed: 3426656]

9. Srivastava S, Ramana KV, Tammali R, Srivastava SK, Bhatnagar A. Contribution of aldose reductase to diabetic hyperproliferation of vascular smooth muscle cells. Diabetes. 2006; 55:901–910. [PubMed: 16567509]

10. Srivastava S. Downregulation of CuZn-superoxide dismutase contributes to beta-adrenergic receptor-mediated oxidative stress in the heart. Cardiovasc Res. 2007; 74:445–455. [PubMed: 17362897]

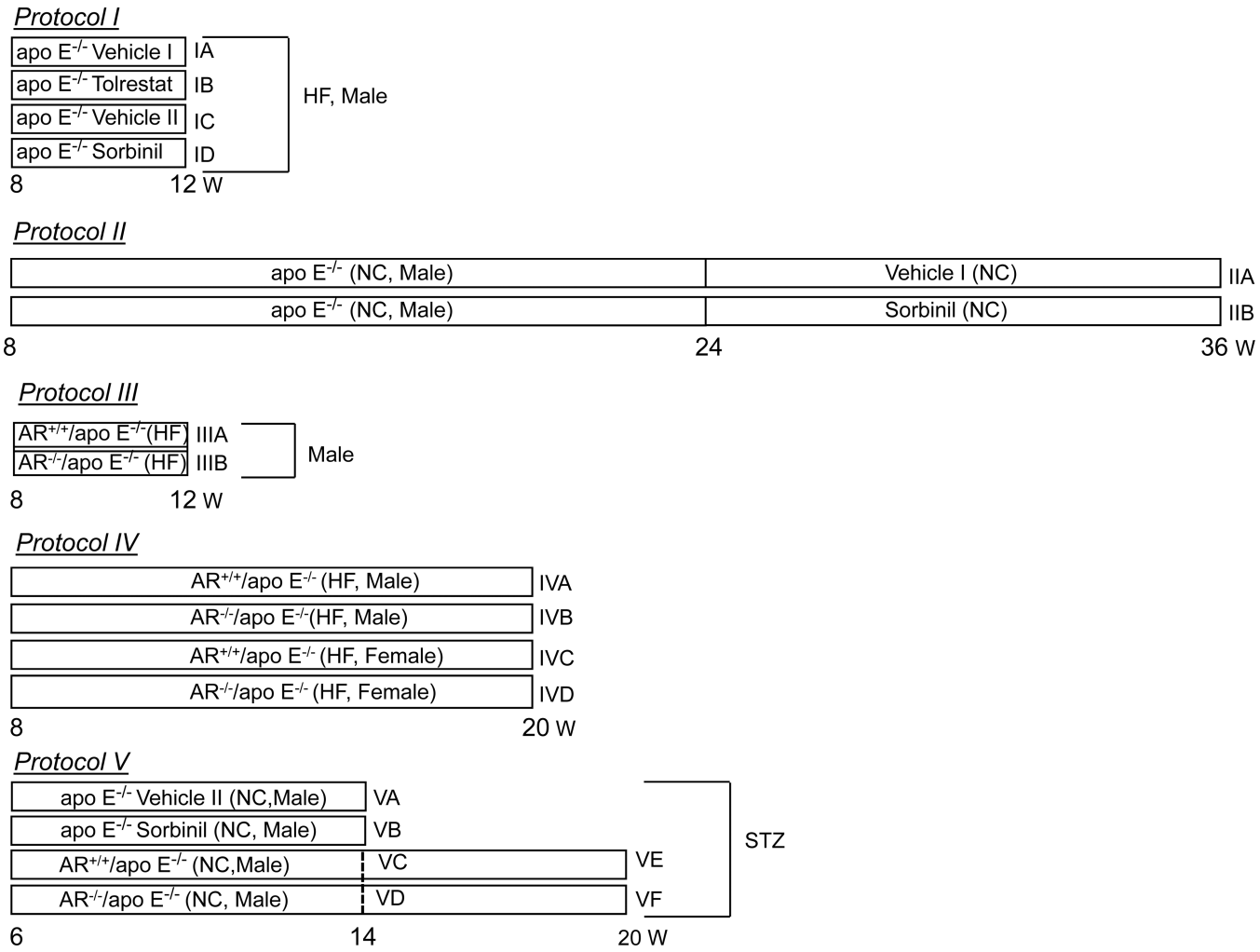

Figure 1.
Treatment protocols of $AR^{-/-}/apoE^{-/-}$ and $AR^{+/+}/apoE^{-/-}$ mice.

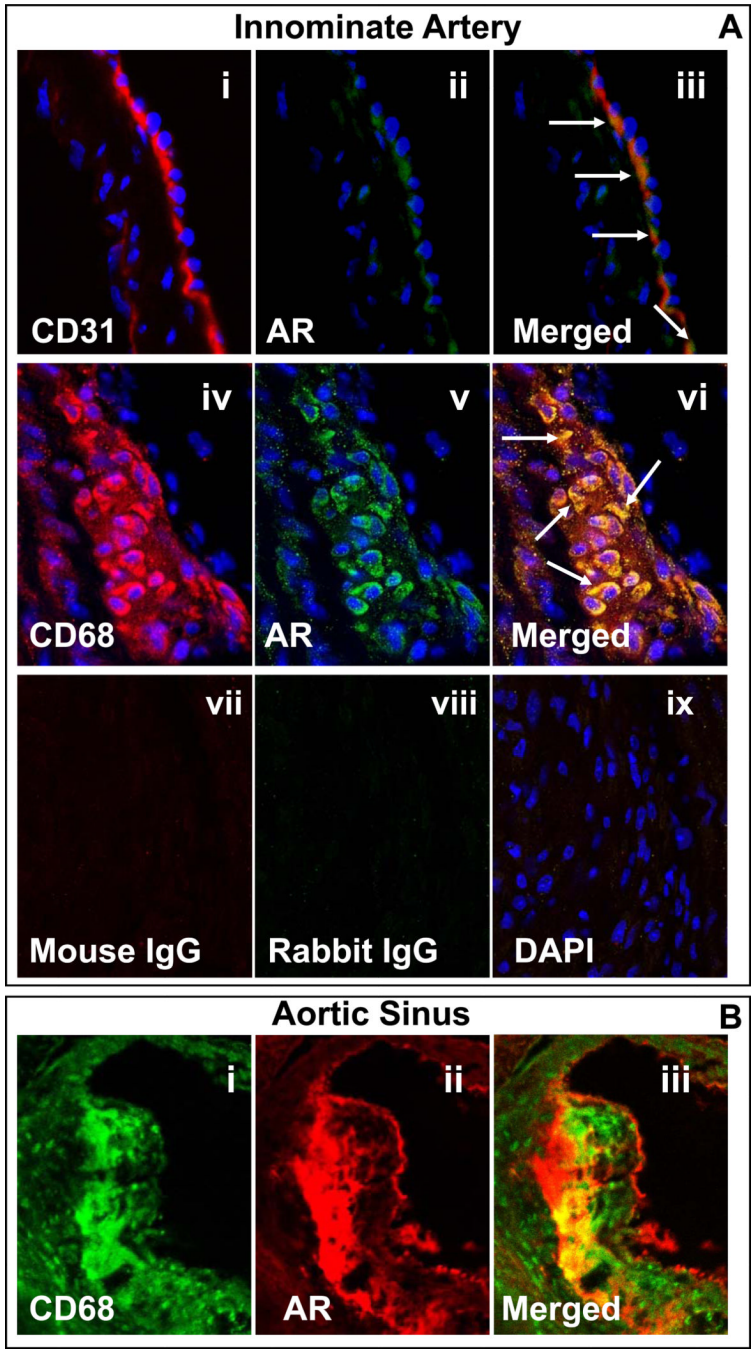

Figure 2.

Expression of AR in the innominate artery and the aortic sinus of apo E-null mice. **A**. Panels (**i–iii**) show the expression and co-localization of AR with endothelial cells in non-diseased innominate arteries. Formalin-fixed cross sections obtained from 8 week-old apoE-null mice, maintained on normal chow were stained with anti- CD31 (**i**; TRITC, red) and aldose reductase (AR; **ii**; Alexa 488, green). The yellow fluorescence in the merged image (**iii**) indicates that AR is expressed in endothelial cells. Panels (**iv–vi**) show the expression and the co-localization of AR with macrophages in the innominate lesions of 20 week old apoE-null mice, maintained on normal chow. Formalin-fixed sections were stained with Alexa 647

conjugated anti-CD68 (**iv**; red) and AR (**v**; green, Alexa 488). The yellow fluorescence in the merged image (**vi**) indicates that AR co-localizes with macrophages. Sections stained with non-immune mouse (**vii**) and rat (**viii**) IgG served as negative control. Nuclei are identified in blue (DAPI; **ix**). Magnification = 630×. **B**. AR co-localizes with macrophages (MOMA-2) in aortic valves. OCT-fixed frozen sections of 20 week old apoE-null mice, maintained on normal chow, were stained with MOMA-2 (**i**; Alexa 488, green) and AR (**ii**; TRITC, red). The yellow fluorescence in the merged image (**iii**) indicates that AR is expressed in significant proportion of macrophages. Magnification = 400×.

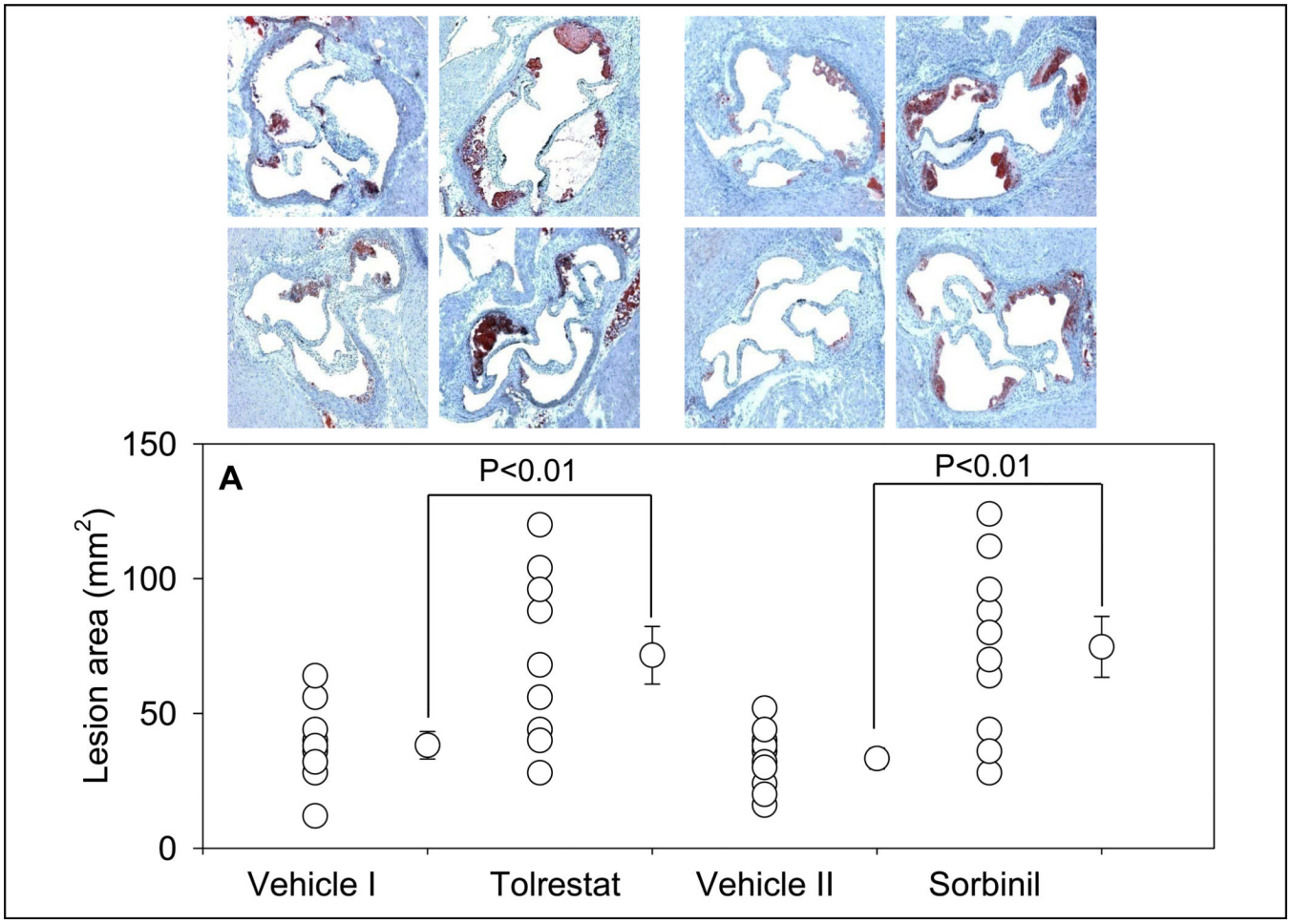

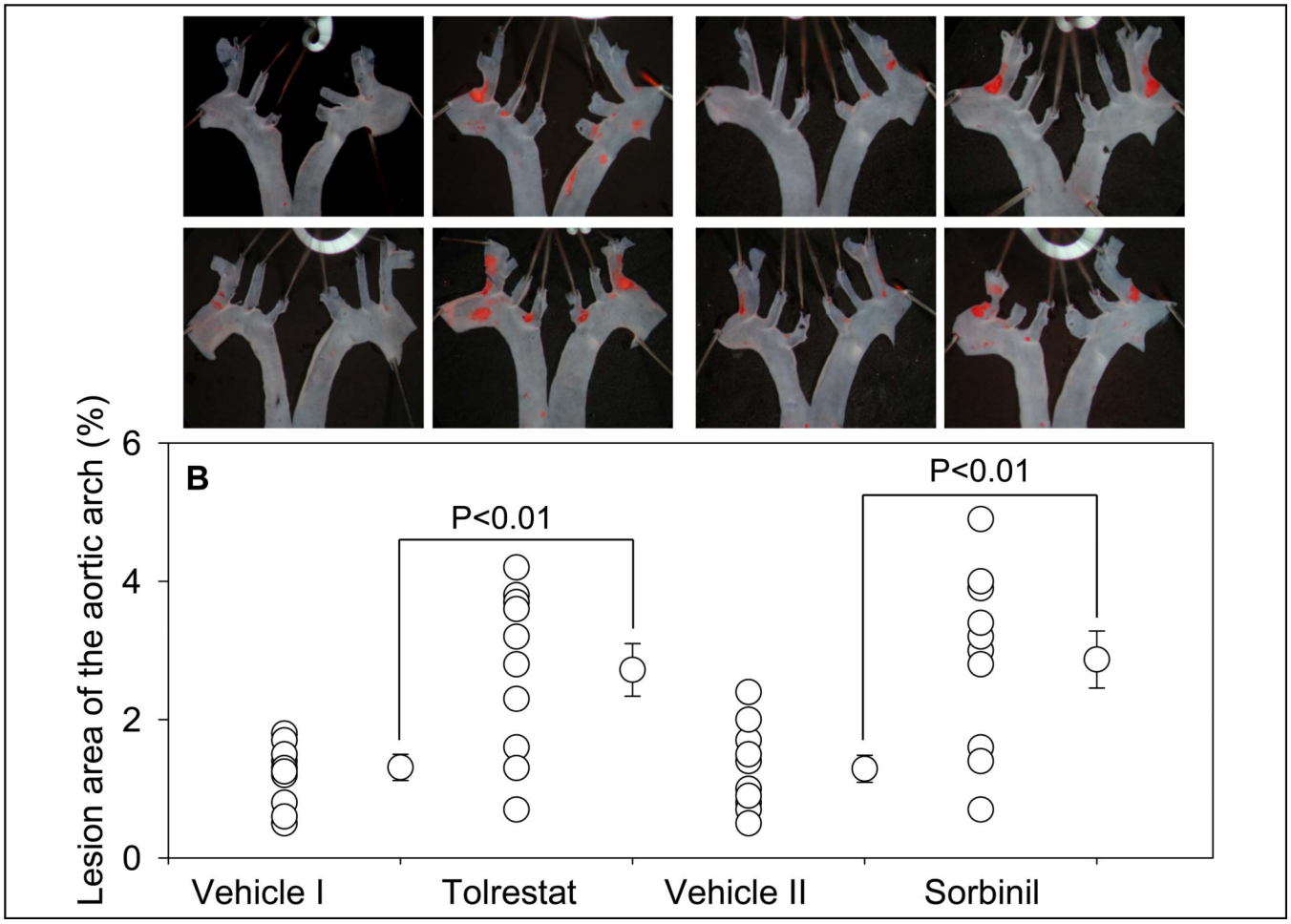

Figure 3.

Inhibition of AR exacerbates early phase of atherogenesis. Eight week old apoE-null mice were fed tolrestat (0.2 g/L in 2.5 mM sodium bicarbonate in drinking water; Protocol IB), or sorbinil (0.2g/L in 0.5 % ethanol in drinking water; Protocol ID) for 4 weeks. Mice fed with the vehicle, 2.5 mM sodium bicarbonate (vehicle I; Protocol IA) or 0.5 % ethanol in drinking water (vehicle II; Protocol IC) served as controls for the tolrestat- or sorbinil-fed mice, respectively. Lesion formation was examined in the aortic sinus (**A**) and the aortic arch (**B**). Lipids were visualized by Oil-Red O staining in the aortic sinus and Sudan IV in the aortic arch. Values are mean ± SEM.

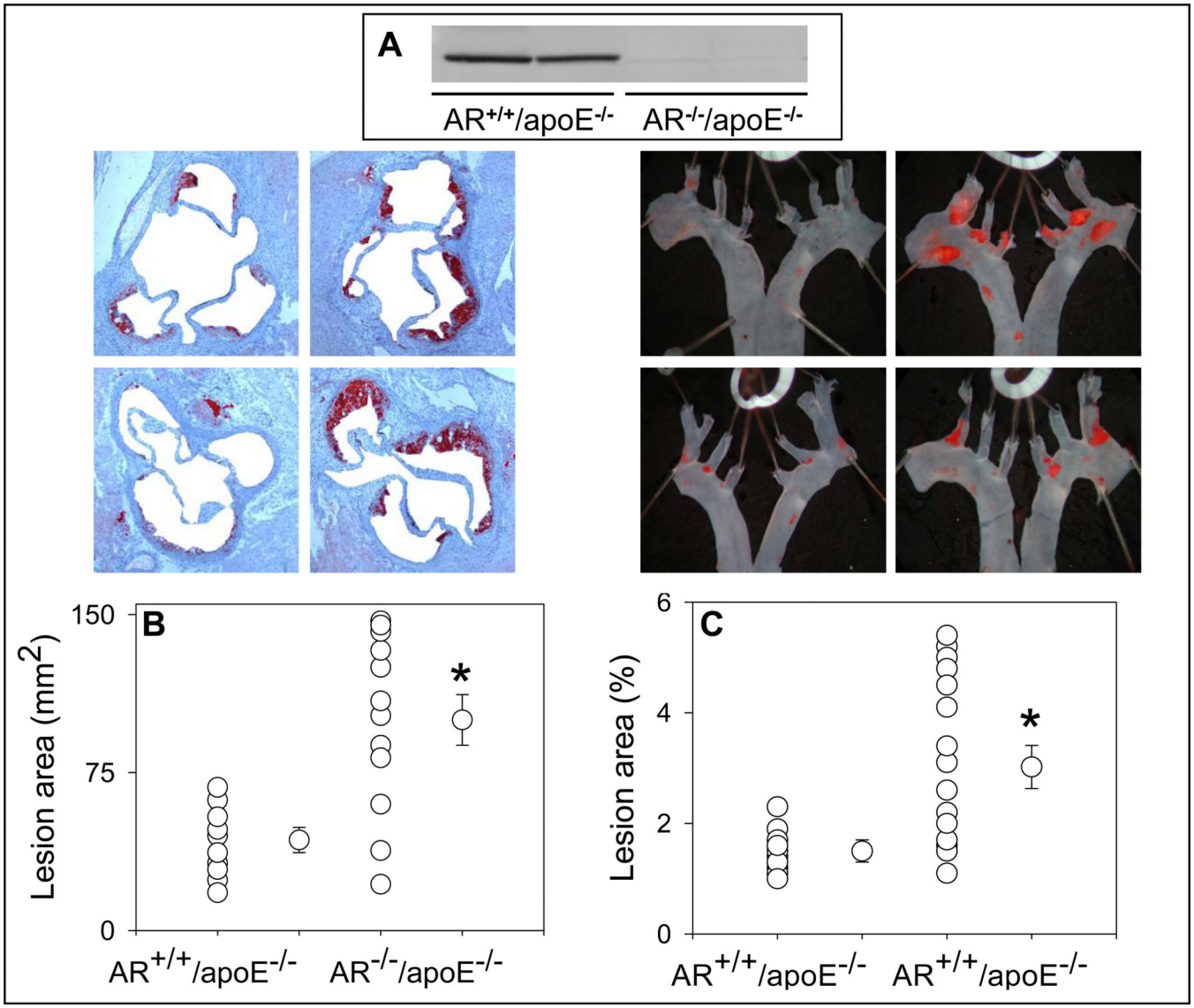

Figure 4.

Genetic ablation of AR exacerbates early phase of atherogenesis. Eight week-old $AR^{-/-}$/$apoE^{-/-}$ and $AR^{+/+}$/$apoE^{-/-}$ mice were maintained on a high- fat diet for 4 weeks (Protocol III). Expression of AR was examined in the heart homogenates by Western blot analysis using anti-AR antibody (**A**). Lesion formation was quantified in the aortic sinus (**B**) and the aortic arch (**C**). In the aortic sinus, lipids were visualized by Oil-Red O staining. Lipids were visualized by Oil-Red O staining in the aortic sinus and Sudan IV in the aortic arch. Values are mean ± SEM. *P < 0.01 versus control.

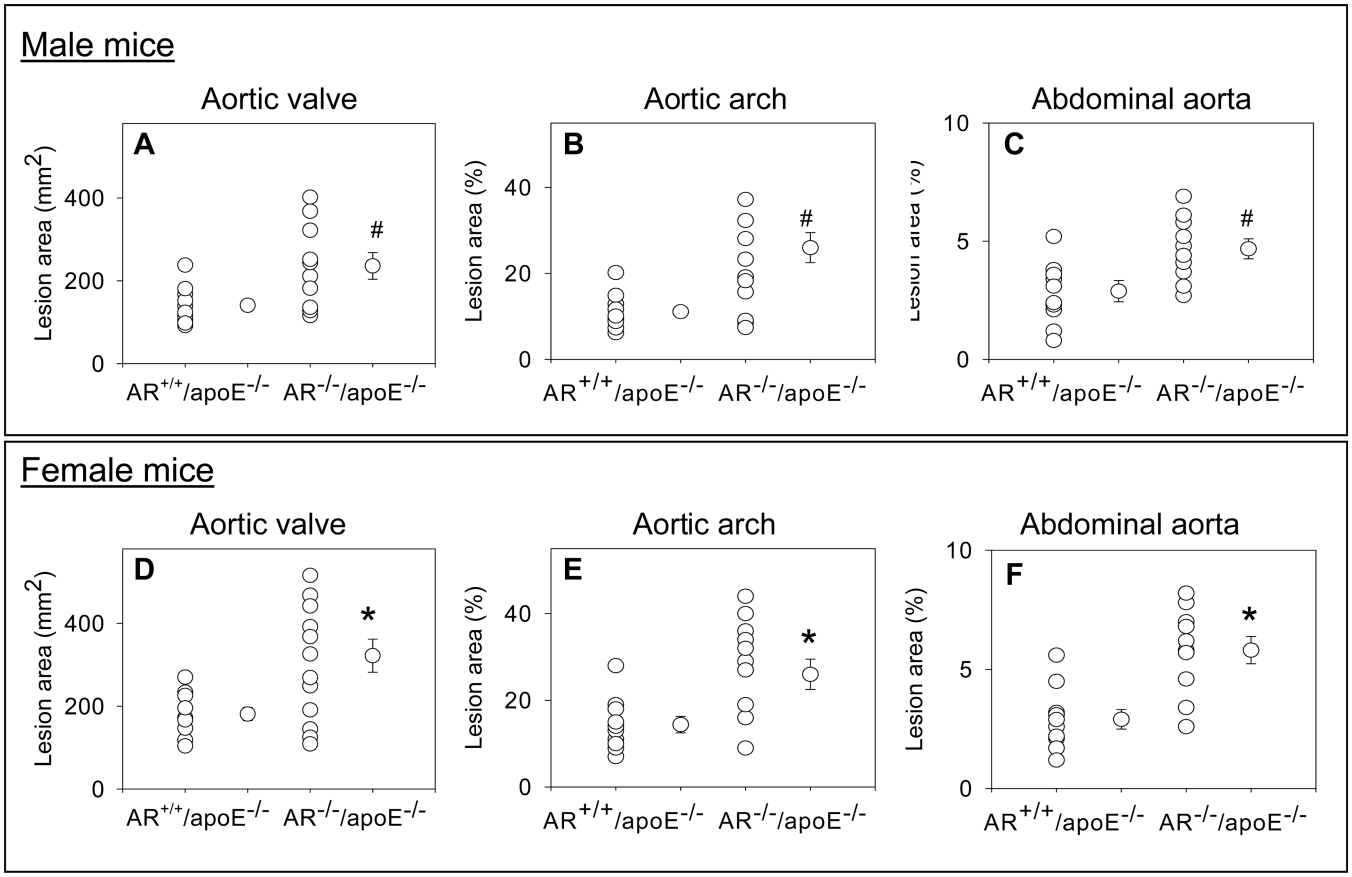

Figure 5.

Genetic ablation of AR exacerbates intermediate lesions. Eight week old $AR^{-/-}/apoE^{-/-}$ and $AR^{+/+}/apoE^{-/-}$ mice were maintained on a high-fat diet for 12 weeks (Protocol IV). Lesion formation in male mice was examined in the aortic sinus (**A**), the aortic arch (**B**) and abdominal aorta (**C**). Panels **D–F** show lesion formation in the aortic sinus, the aortic arch, and the abdominal aorta respectively of female mice. Values are mean ± SEM. *P < 0.01 and # P<0.02 versus controls.

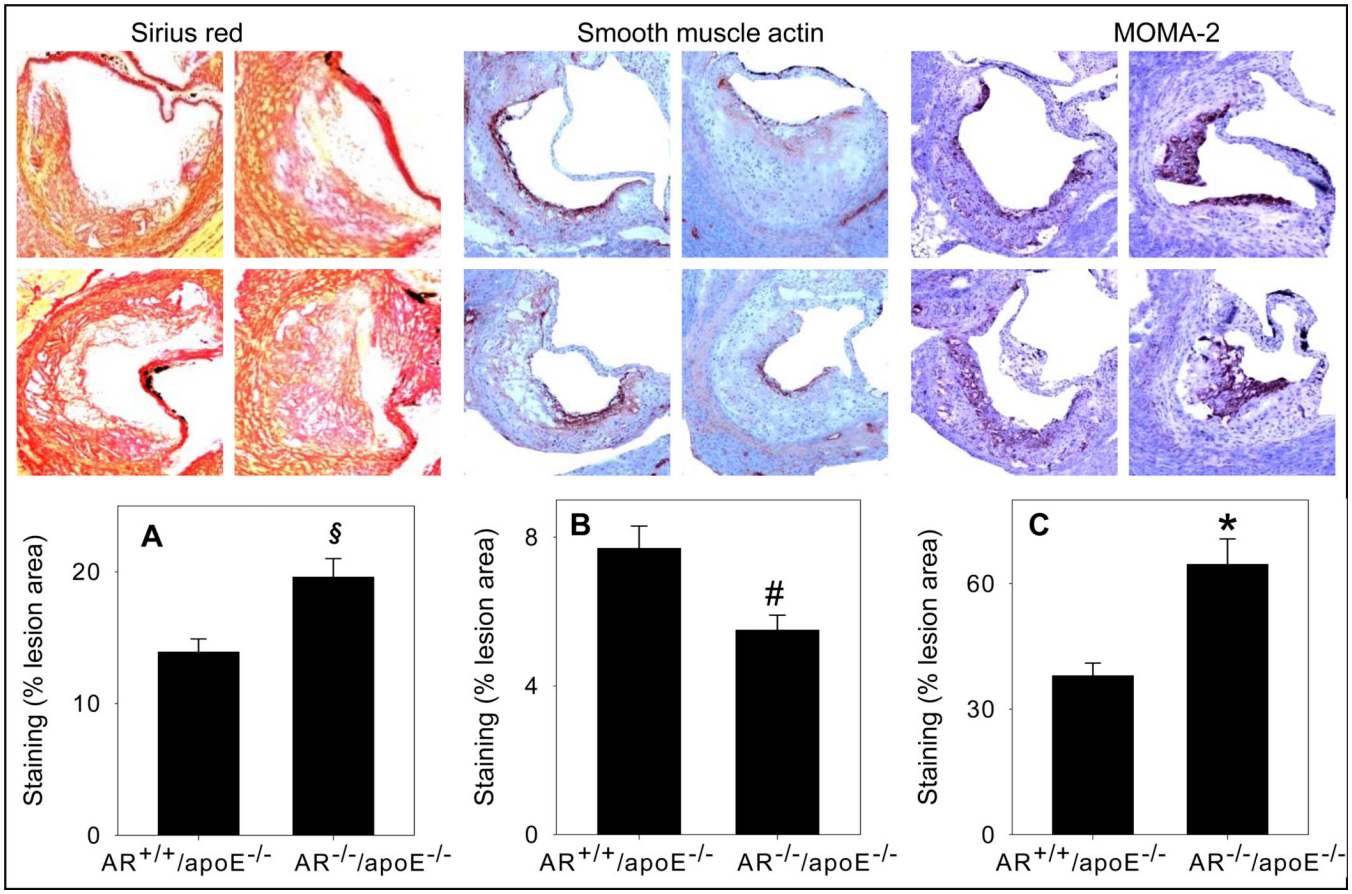

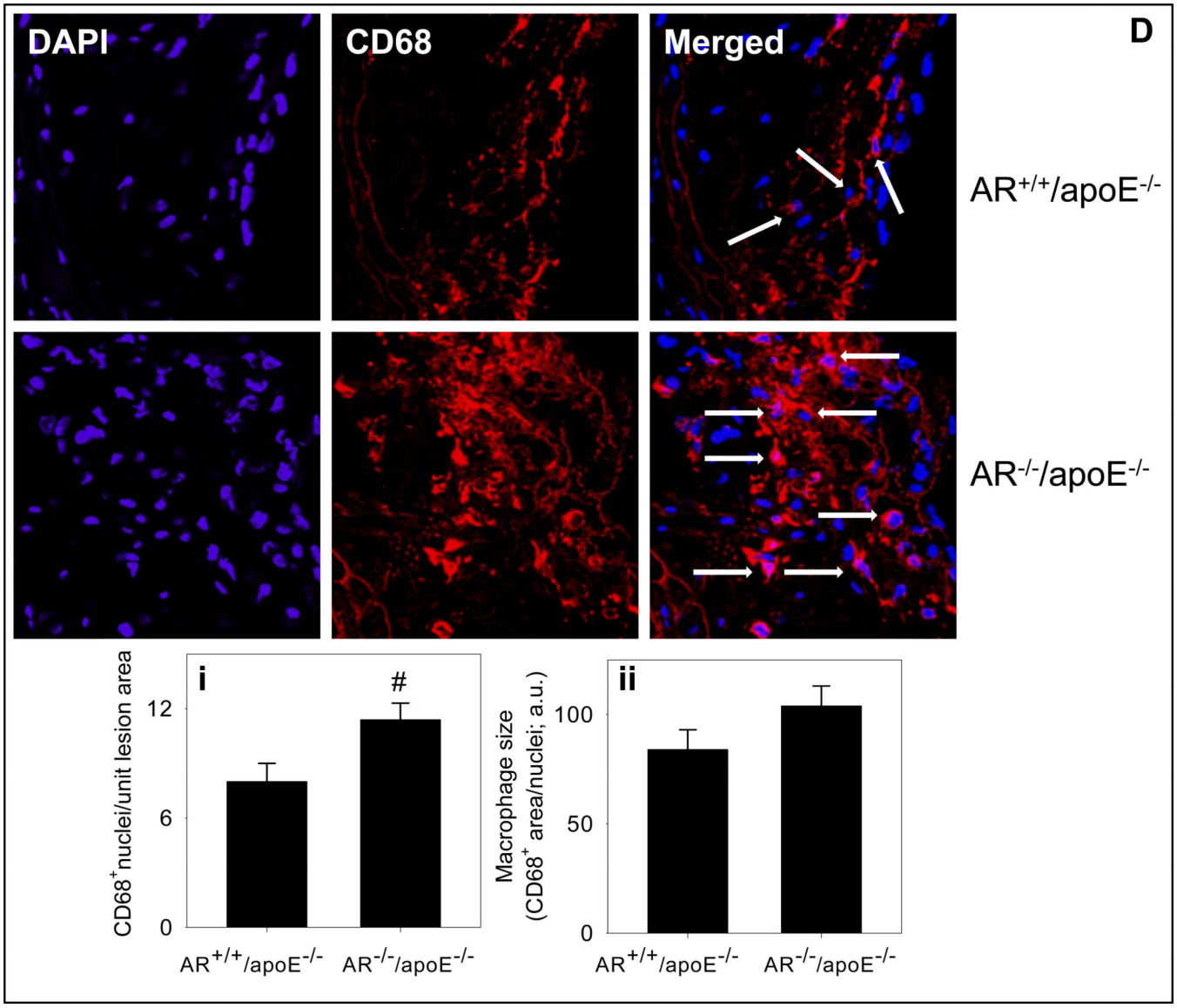

Figure 6.

Genetic ablation of AR affects lesion composition. Female $AR^{-/-}/apoE^{-/-}$ and $AR^{+/+}/apoE^{-/-}$ mice (8 week old) were maintained on high-fat diet for 12 weeks (Protocol IV). Interstitial collagen in the aortic sinus was stained with Sirius Red (**A**). Smooth muscle cells in the aortic roots were visualized with anti-smooth muscle cell actin antibody (**B**).Macrophage accumulation in the aortic sinus was examined by staining with MOMA-2 (**C**) and Alexa 647 conjugated CD-68 (**D**). Nuclei were stained with DAPI (blue). Measurements of $CD68^+$ macrophage number and size are shown in panels **i** and **ii** respectively. Values are mean ± SEM. *P < 0.01, $^{\#}$P<0.02 and §P<0.05 versus controls.

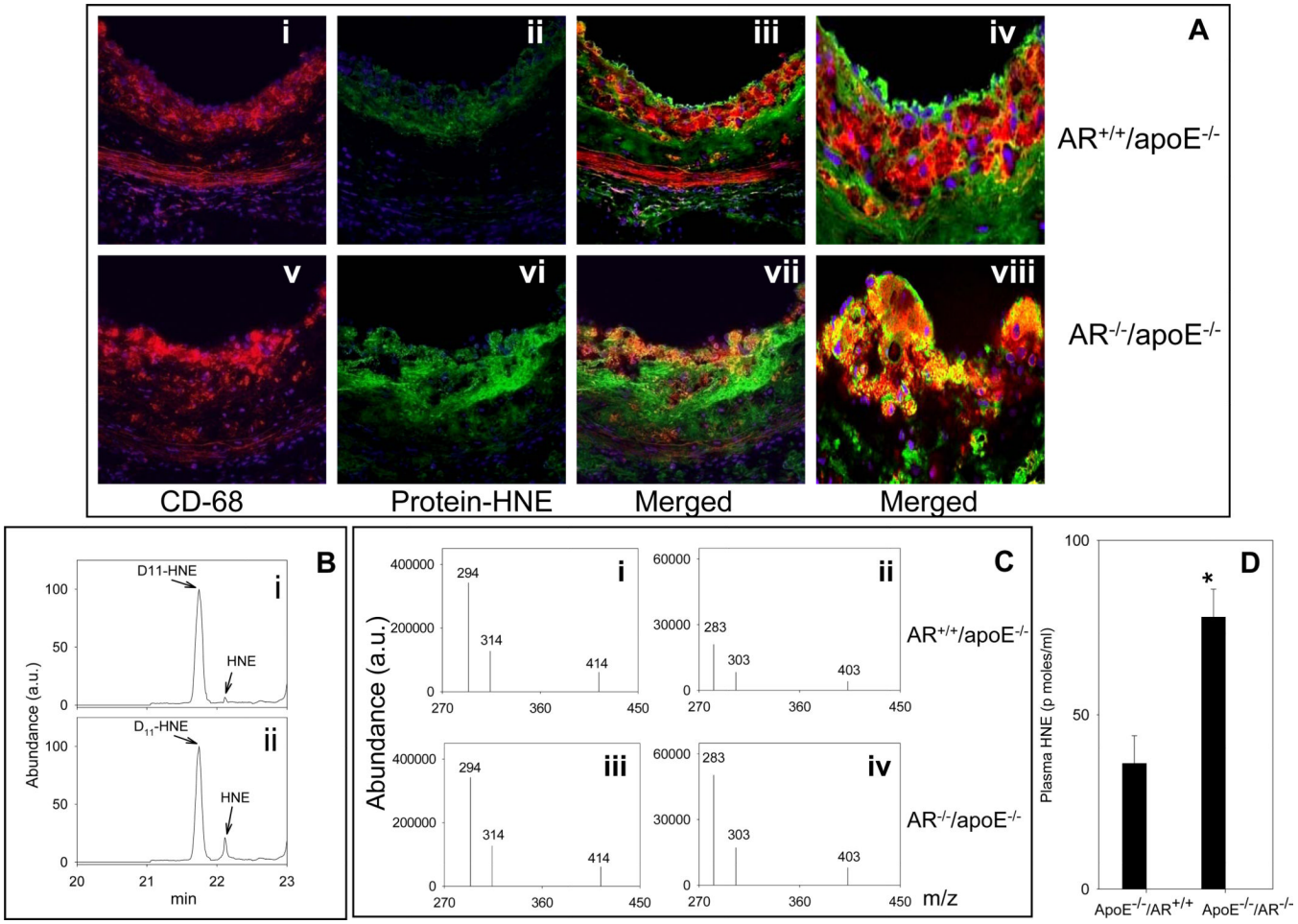

Figure 7.

Genetic ablation of AR increases the accumulation of protein-HNE adducts in the lesions and increases HNE concentration in the plasma. Female $AR^{-/-}/apoE^{-/-}$ and $AR^{+/+}/apoE^{-/-}$ mice (8 weeks old) were maintained on high-fat diet for 12 weeks (Protocol IV). **A.** Sections of the aortic sinus were stained with Alexa 647 conjugated CD68 (red; **i** and **v**) and polyclonal protein-HNE (Alexa 488, green; **ii** and **vi**). The yellow fluorescence in the merged image (**iii** and **vii**) indicates that protein-HNE co-localizes with macrophages. Nuclei are identified in blue (DAPI). Magnification = 400×. Panels **iv** and **viii** show the merged images at 1000× magnification. Plasma HNE was measured by GC-NICI-MS. **B.** Representative chromatogram of the spectrum of HNE in the plasma of $AR^{+/+}/apoE^{-/-}$ (**i**) and $AR^{-/-}/apoE^{-/-}$ mice (**ii**) by select ion monitoring. Panel **C** shows the spectrum of select ions monitored for the quantification of HNE. D_{11}-HNE was used as an internal standard. **D.** The group data for plasma HNE levels. * $P < 0.01$ versus controls.

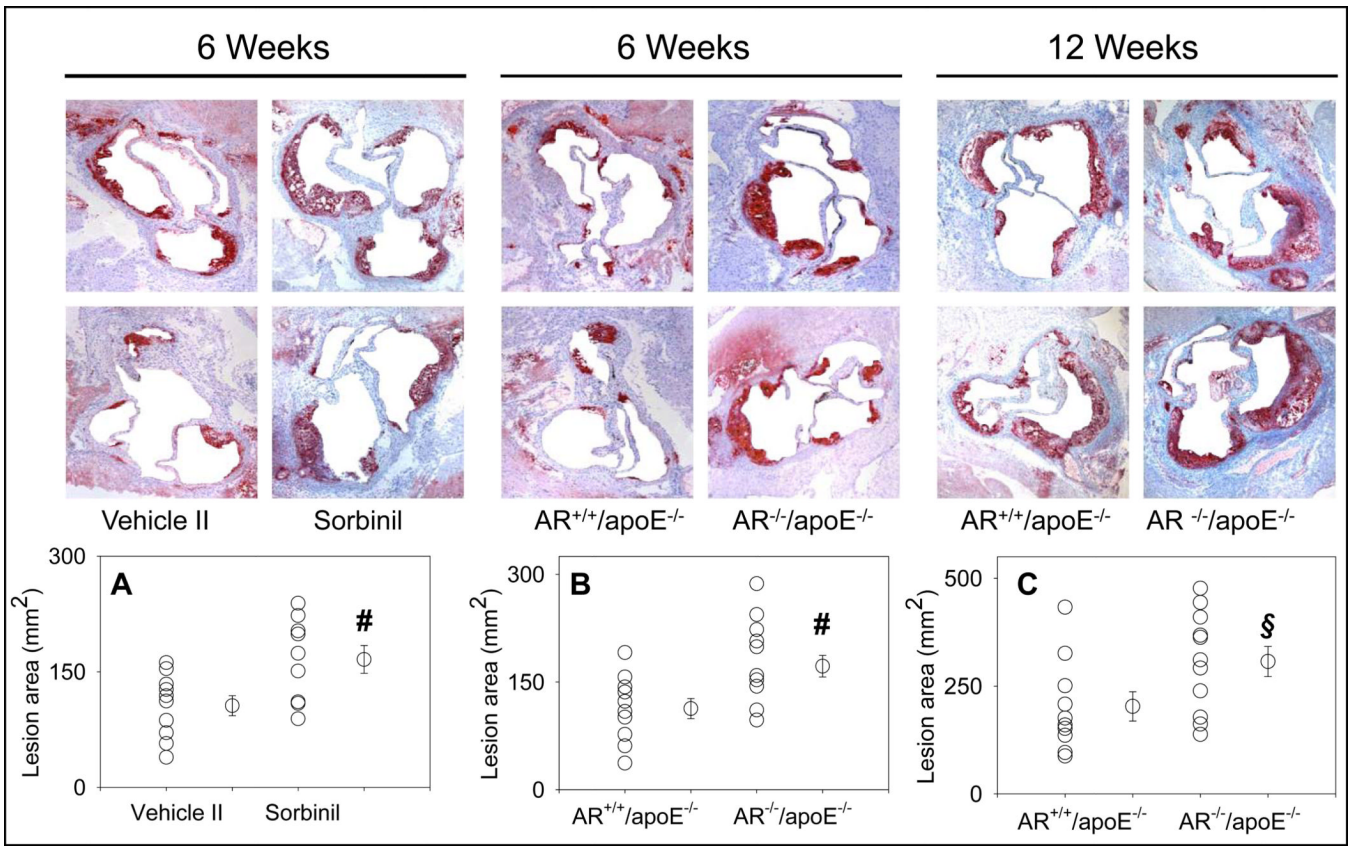

Figure 8.

Pharmacological inhibition and genetic ablation of AR exacerbates atherosclerotic lesion formation in the aortic sinus of diabetic mice. Diabetes was induced in 6- week old mice by 6 daily injections of streptozotocin (65 mg/kg/day; i.p.). At 8 weeks of age, diabetes was verified on the basis of blood glucose level > 250 mg/dL. **A.** Eight weeks old diabetic apoE-null mice were fed sorbinil (0.2g/L in 0.5 % ethanol in drinking water; Protocol VB) for 6 weeks. Vehicle (0.5 % ethanol in drinking water; Protocol VA) fed mice served as controls. Panels **B** and **C** show lesion formation in the aortic sinus of $AR^{-/-}/apoE^{-/-}$ and $AR^{+/+}/apoE^{-/-}$ mice, after 6 (**B**) and 12 (**C**) weeks of diabetes. Lipids were visualized by Oil-Red O staining. Values are mean ± SEM. $^{\#}P<0.02$ and $^{\S}P<0.05$ versus controls.